NANO LETTERS

pubs.acs.org/NanoLett

Letter

Ultrafast Magneto-Optics in Nickel Magnetoplasmonic Crystals

I.A. Novikov, M.A. Kiryanov, P.K. Nurgalieva, A.Yu. Frolov, V.V. Popov, T.V. Dolgova, and A.A. Fedyanin*

Cite This: *Nano Lett.* 2020, 20, 8615–8619

Read Online

ACCESS | Metrics & More | Article Recommendations | Supporting Information

ABSTRACT: Here, we report on ultrafast all-optical modulation of the surface-plasmon (SP)-assisted transverse magneto-optical Kerr effect (TMOKE) and the reflectance in a one-dimensional nickel magnetoplasmonic crystal (MPC). A 50 fs nonresonant laser pump pulse with 7 mJ/cm^2 fluence reduces the magnetization by 65%, which results in the suppression of TMOKE in the SP-resonant probe from 1.15% to 0.4%. The differential reflectance of SP-resonant probe achieves 5.5%. Besides this, it is shown that electron thermalization and relaxation in MPC are several times slower than those in the plane nickel.

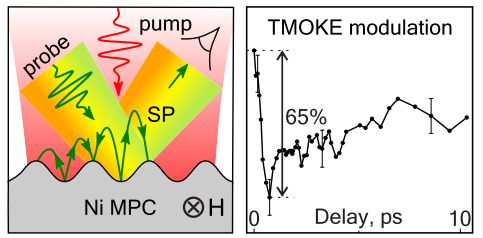

KEYWORDS: *magnetoplasmonics, ultrafast optics, all-optical control, ultrafast demagnetization, electron and spin dynamics, plasmonic crystals*

INTRODUCTION

The nanoscaled structures supporting excitation of surface plasmon (SP) modes have been widely studied for several decades due to their unique properties. They demonstrate strong electromagnetic field localization,[1] great sensitivity to the properties of the surrounding media,[2] optical response modification,[3] as well as magneto-optical response enhancement in magnetoplasmonic crystals[4−8] and metasurfaces.[9] The research resulted in applying plasmonic structures in photovoltaics,[10] sensing,[11,12] integrated photonics,[13,14] and biomedicine.[15] Recently, a new subfield of plasmonics, namely, active plasmonics,[16,17] has emerged. The concept is to tune the SP resonance through an external stimulus such as an electric or magnetic field, mechanical stress, laser radiation, etc. The major advantage of laser radiation is the possibility to modulate the optical response on the subpicosecond time scale comparable with the lifetime of a plasmon[18−20] and the internal processes in the metals such as electron thermalization and electron−phonon relaxation.[21] The modulation of both localized and propagating SPs by laser radiation allows for an efficient ultrafast all-optical switching of intensity and polarization of the incident light.[16,22−24] This phenomenon has been thoroughly studied in plasmonic crystals based on the low-absorptive materials such as gold.[25,26] However, the high-absorptive ferromagnetic magnetoplasmonic crystals have been largely neglected despite the unique steady-state magneto-optical properties they offer.[27−31]

The idea of all-optical modulation is also widely used in the ultrafast control of the magnetic order in the ferromagnetic films.[32−34] The pump-induced modulation of the magnetization state is significantly improved if the magneto-optical active materials are combined with plasmonic nanostructures. Strong localization of the pump pulse by SP excitation reduces the laser fluence required for the ultrafast demagnetization.[35,36] The latter is detected through magneto-optical modulation of the probe pulse which can be also drastically enhanced at the SP resonance.[37]

In this paper, we experimentally study the ultrafast modulation of SP-resonant transverse magneto-optical Kerr effect (TMOKE) induced by a nonresonant 50 fs pump laser pulse in the one-dimensional nickel MPC. The enhancement of magneto-optical effects in the plasmonic structures increases the sensitivity of the ultrafast magnetic processes detection by several orders of magnitude. Besides this, the differential reflectivity measurements reveal the higher laser-induced modulation values and slower relaxation processes in the MPC compared to the plane nickel, due to the modification of the heat diffusion.

RESULTS AND DISCUSSION

The studied magnetoplasmonic crystal was a one-dimensional periodically corrugated nickel surface. It was fabricated using an electron beam lithography and electroplating technique. The MPC surface profile was characterized by atomic force microscopy (AFM). The FFT-processed AFM data revealed the studied sample to have three spatial harmonics and a 94 nm corrugation depth (see the Supporting Information, Section 1). The grating period of 503 ± 2 nm was measured

Received: August 12, 2020
Revised: October 26, 2020
Published: November 25, 2020

https://dx.doi.org/10.1021/acs.nanolett.0c03305
Nano Lett. 2020, 20, 8615−8619

using the optical diffraction method. A 800-μm-thick plane nickel plate was taken as a reference.

As a light source for the reflectance and TMOKE spectral measurements, TM-polarized supercontinuum light generated in the sapphire plate was used. The angle of incidence was 12°. TMOKE was defined as the normalized difference between reflectance at the opposite magnetization directions $R(\pm H)$:

$$\delta = 2\frac{R(+H) - R(-H)}{R(+H) + R(-H)} \quad (1)$$

The value of the magnetic field applied perpendicularly to the plane of incidence was of 500 Oe. Similar measurements were carried out for the reference sample under the same conditions. The results are shown in Figure 1.

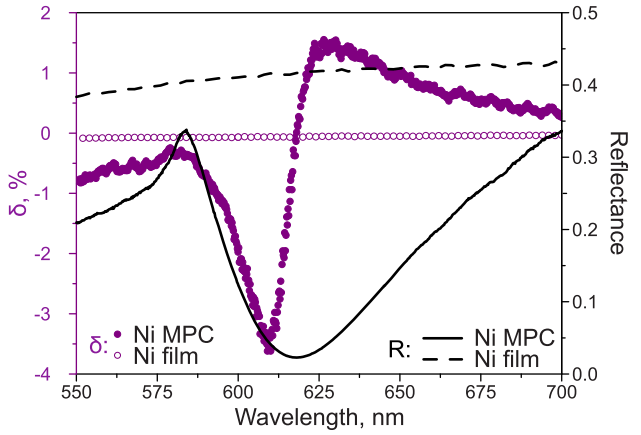

Figure 1. Reflectance (curves) and TMOKE (purple circles) spectra of 1D nickel MPC and plane nickel plate. The incident angle is 12°. TM-polarized light is used.

The MPC reflectance spectrum (black solid curve) has a Fano-type resonance comprising a peak at 580 nm and a dip at 620 nm, while the reference plane nickel plate demonstrates no resonant spectral features at all (black dashed curve). The resonance is associated with the SP excitation in MPC. The spectral peak corresponds to the Rayleigh anomaly, if one of the diffraction orders propagates along the grating surface, while the spectral dip refers to the Wood anomaly, conversion of the incident light into the SP mode. Analytical calculation of the SP dispersion relation shows them to be excited by the -1^{st} diffraction order. The low reflectance values at the wavelength of the dip indicate an almost full energy transfer from the incident light to the SP mode.

The excitation of SP leads to a significant modification of the TMOKE spectrum of MPC and the appearance of the resonant feature that comprises a narrow dip at 610 nm and a broad peak at 630 nm (see Figure 1). Moreover, the TMOKE sign change is observed at the spectral region of a reflectance minimum. Such nonmonotonous TMOKE spectral behavior indicates the SP resonance to be shifted by the magnetic field.[5,27] The absolute TMOKE value as high as 3.6% is achieved in MPC at the wavelength corresponding to the narrow dip in the TMOKE spectrum. At the same wavelength the reference plane plate demonstrates the 0.04% TMOKE value. Thus, the excitation of SP enhances the magneto-optical response of MPC almost by two orders of magnitude.

The measurements of the ultrafast laser-induced reflectance modulation in MPC and the plane nickel plate were carried out in the pump−probe experimental scheme. We used a regeneratively amplified Ti:sapphire laser (Coherent Libra) with 800 nm central wavelength, 50 fs pulse duration, and 1 kHz repetition rate as a source of laser radiation. The 7 mJ/cm^2 pump pulse was directed normally to the studied sample. The laser pulse of such fluence induces the perturbations of electron and lattice temperature that scales linearly with the fluence.[38] The probe was the TM-polarized pulse with a duration up to 95 fs and a central wavelength of 645 nm within the TMOKE Fano resonance (for details, see Supporting Information, Section II). The laser fluence of the probe pulse was about 1 nJ/cm^2. The optical path length was controlled by the delay stage. The spot sizes of the pump and probe pulses on the sample surface were of 800 and 400 μm, respectively.

The differential reflectance $\Delta R/R$ defined as the normalized difference between the reflectance of the excited and the nonexcited sample was measured:

$$\frac{\Delta R}{R}(\tau) = \frac{R_{\text{pump}}(\tau) - R_{\text{no pump}}}{R_{\text{no pump}}} \quad (2)$$

where R_{pump} and $R_{\text{no pump}}$ are the reflectances in the presence and the absence of the pump pulse, respectively, and τ is the pump−probe delay time. The measurements were conducted for the studied non-magnetized MPC and the reference nickel plate. The differential reflectance of the MPC and reference nickel plate is shown in Figure 2.

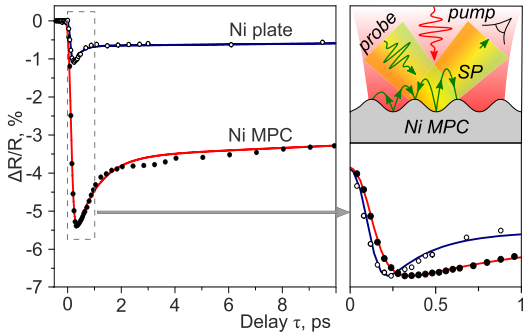

Figure 2. Laser-induced reflectance modulation ($\Delta R/R$) in MPC (solid circles) and the reference plane nickel plate (open circles) at the wavelength of 645 nm. Solid curves represent the analytical fitting of the MPC (red curve) and the reference plate (blue curve) differential reflectance. The inset shows the $\Delta R/R$ values normalized to the maximum in MPC and the nickel plate. Zero delay corresponds to the beginning of the $\Delta R/R$ growth.

The initial reflectance modulation growth arises from the energy transfer from the pump pulse to the free electrons of nickel prolonged by the electron thermalization. This process manifests itself as an energy transfer from the excited electrons of the metal to non-excited ones through the scattering mechanism and usually lasts for several tens of femtoseconds in nickel.[39]

As soon as the thermalization is over, the peak of the reflectance modulation $\Delta R/R$ is reached. Then, the excited electrons start to collide with the phonons of the lattice and give away their energy. This process, known as the electron−phonon relaxation, usually lasts for several hundreds of femtoseconds in nickel.[39] While the system returns to its initial state the differential reflectance $\Delta R/R$ decreases exponentially. Gradually the electron−phonon relaxation

https://dx.doi.org/10.1021/acs.nanolett.0c03305
Nano Lett. 2020, 20, 8615−8619

gives way to the phonon−phonon one. The latter describes the energy redistribution between the phonons of the lattice within several hundreds of picoseconds.

The qualitative analysis of the experimental data reveals the laser-induced reflectance modulation to be different in MPC and the reference plate. MPC demonstrates the maximum differential reflectance $\Delta R/R$ of 5.5% under the 7 mJ/cm^2 fluence. The obtained values of the modulation are comparable to the ones observed in the gold-based plasmonic nanostructures near the d-band transitions for the similar laser fluences.[26] The 5-fold enhancement of $\Delta R/R$ in comparison with the 1.1% effect in the reference nickel plate is explained by the laser-induced modification of the SP wave vector in MPC through its free carrier energy modulation. Moreover, the differential reflectance growth and relaxation times are different in MPC and the reference sample (see the inset in Figure 2). MPC shows a 80 fs $\Delta R/R$ peak retardation relative to the plane nickel plate. This delay indicates the different carrier dynamics inherent to both samples.

The experimentally obtained transient differential reflectances $\Delta R/R$ of the reference nickel plate and MPC can be fitted with the following convolutions:[21,39]

$$\Delta R/R = \exp\left(-\frac{4\ln 2 \times t^2}{\tau_{\text{pump}}^2}\right) \otimes \left[A\left(1 - \exp\left(-\frac{t}{\tau_{\text{ee}}}\right)\right)\exp\left(-\frac{t}{\tau_{\text{ep}}}\right) + B\left(1 - \exp\left(-\frac{t}{\tau_{\text{ep}}}\right)\right)\exp\left(-\frac{t}{\tau_{\text{pp}}}\right)\right] H(t) \otimes \exp\left(-\frac{4\ln 2 \times t^2}{\tau_{\text{probe}}^2}\right) \quad (3)$$

The first convolution describes the optical pumping and the subsequent energy relaxation through electron−electron, electron−phonon, and phonon−phonon scattering. The second convolution refers to the detection of the excited medium via the probe pulse. τ_{pump} and τ_{probe} are the fwhm of the pump and probe Gaussian pulses. τ_{ee}, τ_{ep}, and τ_{pp} are the times of the electron−electron thermalization and the electron−phonon and phonon−phonon relaxations, respectively. The Heaviside step function $H(t)$ limits the exponents' growth at the negative pump−probe delays.

For fitting of the experimental data, it was assumed[40] that $\tau_{\text{probe}} = \tau_{\text{pump}} = 50$ fs. τ_{ee} values extracted from the fit are 35 and 70 fs for the plane nickel plate and MPC, respectively, which is below the temporal resolution of the setup. Thus, we treat them as fitting parameters but not as physical thermalization times. Still, it is clear that the electron thermalization in MPC takes more time than that in plane nickel. The derived electron−phonon relaxation times (τ_{ep}) are of 260 and 800 fs for the reference plane nickel plate and MPC, respectively. The obtained mismatch is associated with the local heating of the electrons in MPC and its surface curvature influence on the electron heat transfer. It will be discussed more thoroughly later. The phonon−phonon relaxation is significantly longer than the considered time scale of 10 ps, and thus, the corresponding process can be neglected in the fit.

The ultrafast magneto-optical measurements were carried out in the TMOKE configuration. The magnetic field of 500 Oe was applied perpendicularly to the plane of the light incidence. To characterize the pump-induced magneto-optical response modulation, the normalized difference between the TMOKE values in the excited $\delta_{\text{pump}}(\tau)$ and the nonexcited $\delta_{\text{no pump}}$ MPC was introduced:

$$\frac{\Delta\delta(\tau)}{\delta} = \frac{\delta_{\text{pump}}(\tau) - \delta_{\text{no pump}}}{\delta_{\text{no pump}}} \quad (4)$$

The laser-induced TMOKE modulation $\Delta\delta/\delta$ in MPC as a function of the pump−probe delay τ is shown in Figure 3 at

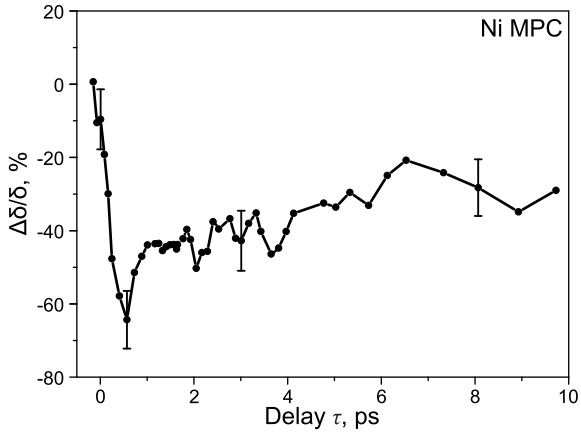

Figure 3. Laser-induced modulation of the SP-enhanced TMOKE in 1D nickel MPC as a function of the pump−probe delay. Zero delay of $\Delta\delta$ matches the $\Delta R/R$ zero delay.

the wavelength of 645 nm. The ultrafast laser heating dampens the steady-state TMOKE by 65 ± 10% within the first several hundreds of femtoseconds. The initial maximal absolute TMOKE value is reduced from 1.15% to 0.4%. The growth of $\Delta\delta/\delta$ is followed by its exponential decrease due to the system relaxation through the electron−phonon and the remagnetization processes. The relaxation occurs within several picoseconds.

The laser-induced absolute TMOKE modulation $\Delta\delta$ cannot exceed the maximal steady-state TMOKE value δ, that is, 4×10^{-4} in plane film (see Figure 1). Thereby, the $\Delta\delta = 0.75 \times 10^{-2}$ in MPC is at least 19 times higher than the corresponding value in the film.

Heating metal by an ultrafast laser pulse changes its dielectric function in two ways, i.e., modifying either its free carrier density (for metals supporting the interband transitions) or energy. The second case may be explained within the Drude model:[41]

$$\epsilon(\omega) = 1 - \frac{\Omega_{\text{p}}^2}{\omega(\omega + i\hbar\gamma_{\text{eff}})} \quad (5)$$

where Ω_{p} and γ_{eff} are the plasma frequency and the effective inverse electron collision time (scattering rate), respectively. The excited (heated) electrons give away their energy in the collisions with the other electrons and phonons. The collision rate is different for the excited and the nonexcited electrons, which results in time-dependent modulation of the metal dielectric function (see eq 5). The dispersion relation of the SP in MPC comprises the dielectric function of the metal:

$$k_{\text{SP}}(\omega) = \frac{\omega}{c}\sqrt{\frac{\epsilon_{\text{m}}\epsilon_{\text{d}}}{\epsilon_{\text{m}} + \epsilon_{\text{d}}}} \quad (6)$$

https://dx.doi.org/10.1021/acs.nanolett.0c03305
Nano Lett. 2020, 20, 8615−8619

where $\epsilon_{m,d}$ are the dielectric functions of the metal and surrounding dielectric, respectively. Thus, the change of the metal dielectric function tunes the SP resonance, i.e., spectrally shifts and broadens, through the modification of the SP wave vector. The tuning of the SP resonance upon the laser pulse is the main reason for high MPC differential reflectance values compared to those observed in the plane Ni plate.

The delay of the differential reflectance peak and significantly longer relaxation time are observed in MPC in comparison with the plane nickel (see Figure 2). To explain the difference, one has to consider the steady-state near-field distribution of the optical pump power absorbed by MPC and electric field localization at the probe wavelength (details can be found in the Supporting Information, Section 3). The surface curvature influences the local heating and hot electron diffusion. The retardation of the probed differential reflectance results from the spatial averaging of the pump-induced nonuniform temperature distribution over the probe field localization area.

The ultrafast TMOKE modulation, shown in Figure 3, can be attributed either to the laser-induced modification of the SP wave vector through the metal dielectric function change, a process that has already been studied here (see Figure 2), or to the ultrafast demagnetization, the rapid decrease of the magnetization on the subpicosecond time scale.[32,42,43] Qualitatively, both mechanisms affect the wave vector of SP propagating in the magnetized medium k_{SP}^{M}:[27]

$$k_{SP}^{M} = k_{SP}\left(1 + \frac{g}{\xi}\right) \tag{7}$$

where k_{SP} is the SP wave vector in the magnetization absence (see eq 6), g is gyration that characterizes the MPC magnetization state, and ξ is the combination of the dielectric functions of metal ϵ_m and the surrounding dielectric ϵ_d also in the magnetization absence. k_{SP}^{M} is a complex value that defines the MPC reflectance and TMOKE. The laser heating modifies the gyration g and the SP wave vector k_{SP} of the MPC. The nonmagnetic pump−probe measurements $\Delta R/R$ reveal that the SP resonance is predominantly shifted upon the pump pulse, similar to the gold-based plasmonic structures case studied earlier.[26] The effect of the laser heating on the SP resonance broadening is relatively small and negligible. Thus, only the real part of the SP wave vector, k_{SP}, is modified. Such change can cause only the spectral shift of the Kerr effect while its amplitude remains the same. However, the ultrafast TMOKE measurement shows the suppression of the Kerr effect in MPC by 65%. As it was stated, the Kerr effect suppression cannot be triggered via the spectral shift of the SP resonance; thus, the only reasonable explanation here is the demagnetization effect.

CONCLUSION

We observe the suppression of TMOKE in the SP-resonant probe from 1.15% to 0.4% by the demagnetization of the nickel MPC under a nonresonant pump. The absolute TMOKE difference is at least 19-fold enhanced in the MPC relative to the plane nickel. It is attributed to the sensitivity of plasmonic systems to magnetization.

The carrier dynamics induced by the ultrashort laser pulse affects the SP excitation process. The laser heating induces the SP wave vector modification through the modulation of the metal optical constants. As a result, a differential reflectivity value as high as 5.5% is achieved in MPC in comparison with 1.1% value in the plane nickel. The electron thermalization and relaxation dynamics are slower in MPC relative to the plane nickel. Electron−phonon relaxation times extracted from the differential reflectance fitting are 800 and 260 fs for the MPC and plane nickel film, respectively. The surface curvature influences the local heating and heat transfer. The retardation of the probed differential reflectance results from the spatial averaging of the pump-induced nonuniform temperature distribution over the probe field localization area.

The results can be applied to the development of the new magnetoplasmonic devices, providing more sensitivity to the magnetic order on the subpicosecond time scale.

ASSOCIATED CONTENT

Supporting Information

The Supporting Information is available free of charge at https://pubs.acs.org/doi/10.1021/acs.nanolett.0c03305.

Details of the sample characterization, estimation of probe pulse duration, and simulation of the pump and probe absorption (PDF)

AUTHOR INFORMATION

Corresponding Author

A.A. Fedyanin − *Faculty of Physics, Lomonosov Moscow State University, 119991 Moscow, Russia;* orcid.org/0000-0003-4708-6895; Email: fedyanin@nanolab.phys.msu.ru

Authors

I.A. Novikov − *Faculty of Physics, Lomonosov Moscow State University, 119991 Moscow, Russia*

M.A. Kiryanov − *Faculty of Physics, Lomonosov Moscow State University, 119991 Moscow, Russia*

P.K. Nurgalieva − *Faculty of Physics, Lomonosov Moscow State University, 119991 Moscow, Russia*

A.Yu. Frolov − *Faculty of Physics, Lomonosov Moscow State University, 119991 Moscow, Russia;* orcid.org/0000-0003-0988-1361

V.V. Popov − *Faculty of Physics, Lomonosov Moscow State University, 119991 Moscow, Russia*

T.V. Dolgova − *Faculty of Physics, Lomonosov Moscow State University, 119991 Moscow, Russia*

Complete contact information is available at: https://pubs.acs.org/10.1021/acs.nanolett.0c03305

Notes

The authors declare no competing financial interest.

ACKNOWLEDGMENTS

We thank Dr. A.A. Ezhov for the AFM measurements and P.A. Kipp for the technical assistance in magneto-optical measurements. The research was supported by the Ministry of Science and Higher Education of the Russian Federation (14.W03.31.0008, experiment), the Russian Foundation for Basic Research (19-02-00876, solid-state characterization of the samples; 20-02-00758, analytical calculations), and the MSU Quantum Technology Center (setup development).

REFERENCES

(1) Barnes, W.; Dereux, A.; Ebbesen, T. Surface Plasmon Subwavelength Optics. *Nature* **2003**, *424*, 824.

(2) Miller, M. M.; Lazarides, A. A. Sensitivity of Metal Nanoparticle Surface Plasmon Resonance to the Dielectric Environment. *J. Phys. Chem. B* **2005**, *109*, 21556.
(3) Fischer, B.; Marschall, N.; Queisser, H. Experimental studies of optical surface excitations. *Surf. Sci.* **1973**, *34*, 50.
(4) Belotelov, V. I.; Akimov, I. A.; Pohl, M.; Kotov, V. A.; Kasture, S.; Vengurlekar, A. S.; Gopal, A. V.; Yakovlev, D. R.; Zvezdin, A. K.; Bayer, M. Enhanced magneto-optical effects in magnetoplasmonic crystals. *Nat. Nanotechnol.* **2011**, *6*, 370.
(5) Grunin, A. A.; Zhdanov, A. G.; Ezhov, A. A.; Ganshina, E. A.; Fedyanin, A. A. Surface-plasmon-induced enhancement of magneto-optical Kerr effect in all-nickel subwavelength nanogratings. *Appl. Phys. Lett.* **2010**, *97*, 261908.
(6) Armelles, G.; Cebollada, A.; García-Martín, A.; González, M. U. Magnetoplasmonics: Combining Magnetic and Plasmonic Functionalities. *Adv. Opt. Mater.* **2013**, *1*, 10.
(7) Rollinger, M.; Thielen, P.; Melander, E.; Östman, E.; Kapaklis, V.; Obry, B.; Cinchetti, M.; García-Martín, A.; Aeschlimann, M.; Papaioannou, E. T. Light Localization and Magneto-Optic Enhancement in Ni Antidot Arrays. *Nano Lett.* **2016**, *16*, 2432.
(8) Maccaferri, N.; Bergamini, L.; Pancaldi, M.; Schmidt, M. K.; Kataja, M.; Dijken, S. v.; Zabala, N.; Aizpurua, J.; Vavassori, P. Anisotropic Nanoantenna-Based Magnetoplasmonic Crystals for Highly Enhanced and Tunable Magneto-Optical Activity. *Nano Lett.* **2016**, *16*, 2533.
(9) Musorin, A. I.; Chetvertukhin, A. V.; Dolgova, T. V.; Uchida, H.; Inoue, M.; Luk'yanchuk, B. S.; Fedyanin, A. A. Tunable multimodal magnetoplasmonic metasurfaces. *Appl. Phys. Lett.* **2019**, *115*, 151102.
(10) Catchpole, K.; Polman, A. Plasmonic solar cells. *Opt. Express* **2008**, *16*, 21793.
(11) Stockman, M. I. Nanoplasmonic sensing and detection. *Science* **2015**, *348*, 287.
(12) Grunin, A. A.; Mukha, I. R.; Chetvertukhin, A. V.; Fedyanin, A. A. Refractive index sensor based on magnetoplasmonic crystals. *J. Magn. Magn. Mater.* **2016**, *415*, 72.
(13) Meinzer, N.; Barnes, W.; Hooper, I. Plasmonic meta-atoms and metasurfaces. *Nat. Photonics* **2014**, *8*, 889.
(14) Ebbesen, T.; Genet, C.; Bozhevolnyi, S. Surface-plasmon circuitry. *Phys. Today* **2008**, *61*, 44.
(15) Willets, K.; Van Duyne, R. Localized Surface Plasmon Resonance Spectroscopy and Sensing. *Annu. Rev. Phys. Chem.* **2007**, *58*, 267.
(16) Temnov, V. V. Ultrafast acousto-magneto-plasmonics. *Nat. Photonics* **2012**, *6*, 728.
(17) Jiang, N.; Zhuo, X.; Wang, J. Active Plasmonics: Principles, Structures, and Applications. *Chem. Rev.* **2018**, *118*, 3054.
(18) Ropers, C.; Park, D. J.; Stibenz, G.; Steinmeyer, G.; Kim, J.; Kim, D. S.; Lienau, C. Femtosecond Light Transmission and Subradiant Damping in Plasmonic Crystals. *Phys. Rev. Lett.* **2005**, *94*, 113901.
(19) Vengurlekar, A. S.; Gopal, A. V.; Ishihara, T. Femtosecond pulse distortion at surface plasmon resonances in a plasmonic crystal: Effect of surface plasmon lifetime. *Appl. Phys. Lett.* **2006**, *89*, 181927.
(20) Afinogenov, B. I.; Bessonov, V. O.; Soboleva, I. V.; Fedyanin, A. A. Ultrafast All-Optical Light Control with Tamm Plasmons in Photonic Nanostructures. *ACS Photonics* **2019**, *6*, 844.
(21) Sun, C.-K.; Vallée, F.; Acioli, L.; Ippen, E. P.; Fujimoto, J. G. Femtosecond investigation of electron thermalization in gold. *Phys. Rev. B: Condens. Matter Mater. Phys.* **1993**, *48*, 12365.
(22) Taghinejad, M.; Cai, W. All-Optical Control of Light in Micro- and Nanophotonics. *ACS Photonics* **2019**, *6*, 1082.
(23) Zhang, X.; Yang, J. Ultrafast Plasmonic Optical Switching Structures and Devices. *Front. Phys.* **2019**, *7*, 190.
(24) Bossini, D.; Belotelov, V. I.; Zvezdin, A. K.; Kalish, A. N.; Kimel, A. V. Magnetoplasmonics and Femtosecond Optomagnetism at the Nanoscale. *ACS Photonics* **2016**, *3*, 1385.
(25) Pohl, M.; Belotelov, V. I.; Akimov, I. A.; Kasture, S.; Vengurlekar, A. S.; Gopal, A. V.; Zvezdin, A. K.; Yakovlev, D. R.; Bayer, M. Plasmonic crystals for ultrafast nanophotonics: Optical switching of surface plasmon polaritons. *Phys. Rev. B: Condens. Matter Mater. Phys.* **2012**, *85*, No. 081401.
(26) Rotenberg, N.; Betz, M.; van Driel, H. Ultrafast control of grating-assisted light coupling to surface plasmons. *Opt. Lett.* **2008**, *33*, 2137.
(27) Chetvertukhin, A. V.; Grunin, A. A.; Baryshev, A. V.; Dolgova, T. V.; Uchida, H.; Inoue, M.; Fedyanin, A. A. Magneto-optical Kerr effect enhancement at the Wood's anomaly in magnetoplasmonic crystals. *J. Magn. Magn. Mater.* **2012**, *324*, 3516.
(28) Belyaev, V. K.; Rodionova, V. V.; Grunin, A. A.; Inoue, M.; Fedyanin, A. A. Magnetic field sensor based on magnetoplasmonic crystal. *Sci. Rep.* **2020**, *10*, 7133.
(29) Frolov, A. Y.; Shcherbakov, M. R.; Fedyanin, A. A. Dark mode enhancing magneto-optical Kerr effect in multilayer magneto-plasmonic crystals. *Phys. Rev. B: Condens. Matter Mater. Phys.* **2020**, *101*, 045409.
(30) Tran, N.-M.; Chioar, I.-A.; Stein, A.; Alekhin, A.; Juvé, V.; Vaudel, G.; Razdolski, I.; Kapaklis, V.; Temnov, V. Observation of the nonlinear Wood's anomaly on periodic arrays of nickel nanodimers. *Phys. Rev. B: Condens. Matter Mater. Phys.* **2018**, *98*, 245425.
(31) Maccaferri, N.; Inchausti, X.; García-Martín, A.; Cuevas, J. C.; Tripathy, D.; Adeyeye, A. O.; Vavassori, P. Resonant Enhancement of Magneto-Optical Activity Induced by Surface Plasmon Polariton Modes Coupling in 2D Magnetoplasmonic Crystals. *ACS Photonics* **2015**, *2*, 1769.
(32) Beaurepaire, E.; Merle, J.-C.; Daunois, A.; Bigot, J.-Y. Ultrafast Spin Dynamics in Ferromagnetic Nickel. *Phys. Rev. Lett.* **1996**, *76*, 4250.
(33) Guidoni, L.; Beaurepaire, E.; Bigot, J.-Y. Magneto-optics in the Ultrafast Regime: Thermalization of Spin Populations in Ferromagnetic Films. *Phys. Rev. Lett.* **2002**, *89*, 017401.
(34) Carpene, E.; Mancini, E.; Dallera, C.; Brenna, M.; Puppin, E.; De Silvestri, S. Dynamics of electron-magnon interaction and ultrafast demagnetization in thin iron films. *Phys. Rev. B: Condens. Matter Mater. Phys.* **2008**, *78*, 174422.
(35) Xu, H.; Hajisalem, G.; Steeves, G. M.; Gordon, R.; Choi, B. C. Nanorod Surface Plasmon Enhancement of Laser-Induced Ultrafast Demagnetization. *Sci. Rep.* **2015**, *5*, 15933.
(36) Kataja, M.; Freire-Fernandez, F.; Witteveen, J. P.; Hakala, T. K.; Torma, P.; van Dijken, S. Plasmon-induced demagnetization and magnetic switching in nickel nanoparticle arrays. *Appl. Phys. Lett.* **2018**, *112*, 072406−1.
(37) Shcherbakov, M. R.; Vabishchevich, P. P.; Frolov, A. Y.; Dolgova, T. V.; Fedyanin, A. A. Femtosecond intrapulse evolution of the magneto-optic Kerr effect in magnetoplasmonic crystals. *Phys. Rev. B: Condens. Matter Mater. Phys.* **2014**, *90*, 201405.
(38) Wellershoff, S.-S.; Hohlfeld, J.; Gudde, J.; Matthias, E. The role of electron-phonon coupling in femtosecond laser damage of metals. *Appl. Phys. A: Mater. Sci. Process.* **1999**, *69*, S99.
(39) van Kampen, M.; Kohlhepp, J.; Jonge, W.; Koopmans, B.; Coehoorn, R. Subpicosecond electron and phonon dynamics in nickel. *J. Phys.: Condens. Matter* **2005**, *17*, 6823.
(40) Hopkins, P. E.; Klopf, J. M.; Norris, P. M. Influence of interband transitions on electron-phonon coupling measurements in Ni films. *Appl. Opt.* **2007**, *46*, 2076.
(41) Ashcroft, N.; Mermin, N. *Solid State Physics*; Saunders College Publishing and Harcourt College Publishing: Philadelphia, 1976.
(42) Kirilyuk, A.; Kimel, A.; Rasing, T. Ultrafast optical manipulation of magnetic order. *Rev. Mod. Phys.* **2010**, *82*, 2731.
(43) Koopmans, B.; Malinowski, G.; Dalla Longa, F.; Steiauf, D.; Fähnle, M.; Roth, T.; Cinchetti, M.; Aeschlimann, M. Explaining the paradoxical diversity of ultrafast laser-induced demagnetization. *Nat. Mater.* **2010**, *9*, 259.

https://dx.doi.org/10.1021/acs.nanolett.0c03305
Nano Lett. 2020, 20, 8615−8619